RSC Advances

ROYAL SOCIETY OF CHEMISTRY

www.rsc.org/advances

Polymer composite random lasers based on diatom frustules as scatterers

Francesca Romana Lamastra[1], Roberta De Angelis[1,2], Alessandra Antonucci[3,4], Damiano Salvatori[2], Paolo Prosposito[1,2], Mauro Casalboni [1,2], Roberta Congestri[4], Sonia Melino[5], Francesca Nanni[1,6]*

[1]*Italian Interuniversity Consortium on Materials Science and Technology (INSTM), Research Unit Roma Tor Vergata, Via del Politecnico 1- 00133 Rome, Italy*
[2]*Department of Industrial Engineering, University of Rome 'Tor Vergata', Via del Politecnico 1- 00133, Rome, Italy*
[3]*Department of Environmental, Biological and Pharmaceutical Sciences and Technologies – Second University of Naples, Via Vivaldi, 43 - 81100 Caserta, Italy*
[4]*Department of Biology, University of Rome 'Tor Vergata', Via della Ricerca scientifica, 1- 00133 Rome, Italy*
[5]*Department of Chemical Sciences and Technologies, University of Rome 'Tor Vergata', Via della Ricerca scientifica, 1- 00133 Rome, Italy*
[6]*Department of Enterprise Engineering, University of Rome Tor Vergata, Via del Politecnico 1- 00133 Rome, Italy*

**Corresponding author*

Telephone: +39 06 72594495; Fax: +39 06 72594328

E-mail: lamastra@scienze.uniroma2.it

Abstract

In this work the possibility to exploit the ability of multiple scattering and localization of light shown by the diatom silica shells (frustules), for the photoluminescence amplification in a random laser was investigated. To this aim polymethylmethacrylate matrix composite random lasers based on rhodamine B and frustules as gain medium and scatterers, respectively, were prepared by solvent casting. Two different kinds of frustules were used, the first represented by diatomite, fossil material composed by a mixture of frustules from different diatom species, without specific shape, size and porosity; The second were living diatom frustules from freshwater biofilm, a more homogeneous biosilica, dominated by one frustule type.

Chemical properties, morphology and photoluminescence of both biosilica fillers were investigated. Random laser experiments were carried out on polymer composites. Diatomite material was characterised by rectangular and circular pores, ranging from 25 nm to 1 μm in size and showed weak photoluminescence upon excitation at 405 nm. Biofilm frustules were more homogeneous in size and microstructure, with average length of about 20 μm and pore diameters between 20 and 100 nm. These frustule photoluminescence, observed after irradiation at 488, 515, 543 and 635 nm

was higher than in diatomite. In addition, the two biosilica material differed with respect to the presence of superficial silanol groups, that were not detected in diatomite. Random Laser experiments showed incoherent random lasing effect in all polymer composites. The laser threshold diminished at increasing frustule content, with a lowest value recorded using biofilm frustules (308 kW/cm^2). This is probably due to the frustule size exhibited in this almost monospecific biosilica, that was in the range of most typical morphology-dependent resonators.

Keywords: Photoluminescence; Nanostructured pores; Diatom frustules; Random laser.

1. Introduction

Diatoms are highly successful photosynthetic microorganisms colonising every aquatic environment, they possess multipartite silica shells exhibiting unique micro- and nano-porous architectures, which contribute to high surface area. Frustules also display efficient photoluminescence within the visible spectrum along with a good mechanical strength.[1-3]

Hierarchical organisation of diatom frustule is exactly reproduced by the billion during diatom vegetative growth at the expense of only solar energy, water, atmospheric CO_2 and minerals abundant in nature. Recently, light has been shed on optical, photonic and microfluidic properties of the quasi periodic frustule structure opening new paths in nanotechnological application and materials science.[4-7] These efforts have provided more opportunities to use biosilica structures in microsystems and other commercial products, in particular, given the capability of frustules of interacting with light they have been explored for application as photoanodes in dye sensitised solar cells (DSSCs)[8], in the biomanufacture field of silica-titania photocatalysts for NOx abatement and air purification under UV radiation, and also in biomedical applications.[9-11] Frustules have been shown to act as photonic crystals for gas sensing, chemically modified frustules can properly bind highly selective bioprobes such as an antibody based on photoluminescence (PL)[12] and can be used as advanced probes for holographic optical tweezing application.[13]

Luminescence activity of diatom frustules is related to (i) surface oxygen vacancies states which may act as excited states for radiative transitions,[12] (II) surface silanol groups and their distribution on the frustule fine structures, (III) pore arrays at the micro- to nano-meter scale.[14] However, no studies have yet tested frustule effect in random laser technology, although diatom nanostructured biosilica is a low-cost material and a by-product of monospecific diatom mass cultivation for added value compound production.[15-18]

A random laser is a system formed by a random assembly of elastic scatterers dispersed into an optical gain medium. The multiple scattering of photons replaces the standard optical cavity of

traditional lasers and the interplay between gain and scattering determines the lasing properties. [19,20] The light that is generated into a strongly scattering active medium makes a long random walk before it can leave the medium and can be significantly amplified in between the scattering events. This is an intensity feedback and lead to the so-called incoherent random laser (RL) effect. In this case above a certain pumping threshold the spectral narrowing occurs at a single frequency close to the center frequency of the amplification line of the active medium (close to the maximum of the spontaneous emission band), and the spectra is relatively broad (with typical full width at half maximum (FWHM) of about 4 nm).[21] When the transport mean free path (the average distance the light travels in between two scattering events) approaches the optical wavelength a different feedback mechanism takes place. In this case after multiple scattering light returns to a scatterer from which it has been scattered before, thus forming a loop which reinforces some resonant frequencies. In this process the random laser is said to be coherent and above the lasing threshold the emission spectrum shows a series of discrete narrow peaks (with FWHM of few Å).[22] So far random laser action has been reported for different materials including powders,[23,24] liquid solutions of dyes and particles (both dielectric and metallic)[21] and dye doped polymeric composite materials with embedded scattering particles.[25] Among these materials RL polymer composites present numerous advantages like the low fabrication cost, sample specific wavelength of operation, flexible shape and compatibility with a wide range of substrate materials that hold great promise for a variety of applications. Examples include a laser paint that can be coated on screws, nuts, bolts and manufactured parts for machine-vision[21] or serve as a rugged and low-cost method of identification for downed ships, aircraft and satellites.[26]

In this work we explored the multiple light scattering shown by diatom frustules in order to amplify the photoluminescence in a random laser. To this aim Poly(methylmethacrylate)/rhodamine B (PMMA/RhB) matrix composites with frustules as filler were prepared and their lasing action investigated. RhB, which is a dye belonging to the xanthene family widely employed in various spectroscopic studies was chosen as the optically active material.

2. Experimental

2.1 Materials

PMMA with MW 350000, and dye RhB *for fluorescence characterisation* (RhB) were purchased from Aldrich and used as received, without further treatment. Chloroform (ACS reagent) was used as solvent.

In order to investigate how different scatterer morphologies and porosity affect the lasing action two different kinds of frustules were used:

- diatomite (DE) (*Celite® Analytical Filter Aid II* (CAFA II), Aldrich) used without any further purification. Which is a mineral assemblage mostly consisting of frustules of sedimented dead diatoms of different species and some other minerals such as clay minerals and feldspar.[27] It has been widely used as filter aid, porous support for chemical catalysts and adsorbent for liquids.[28]
- frustules of living diatoms (*Nitzschia palea* var. *minuta*, as dominant species, and small amounts of *N. amphibia*, *N. umbonata* and *Eolimna subminuscola*), obtained from phototrophic biofilms collected in a wastewater treatment plant for municipal wastes (where a limited number of pennate diatoms have been previously shown to proliferate[29,30] located at Furbara (Rome, Italy). Biofilms were treated with a hot mixture of H_2SO_4: HNO_3: H_2O = 3:1:1 in order to remove the organic component. The resulting biosilica was then preserved in ethyl alcohol. These frustules, obtained from living biofilms, are referred to as FUR throughout the text.

2.2 Preparation of random laser based on diatom frustules as scatterers

PMMA/RhB matrix composites with frustules as filler (3-20 wt% with respect to the polymer) were prepared by solvent casting. Frustules were dispersed in a chloroform solution of RhB ($1.95 \cdot 10^{-4}$ M) by means of sonication for 80 minutes. Then, PMMA (60 mg/ml) was dissolved in the previous prepared dispersion under stirring for 4 h at room temperature. The resulting mixtures were poured into a Teflon Petri dish and dried at RT.

As reference, PMMA/RhB samples were also prepared. All samples realised and their nomenclature are reported in **Table 1**.

Table 1
Summary and labelling of all prepared samples

Nomenclature	Type of frustules	Content of frustules (wt. % with respect to the polymer matrix)	Content of RhB (wt. % with respect to the polymer matrix)
PMMA/RhB/DE0	-	0	0.155%
PMMA/RhB/DE3	DE	3%	0.155%
PMMA/RhB/DE5	DE	5%	0.155%
PMMA/RhB/DE7	DE	7%	0.155%
PMMA/RhB/DE20	DE	20%	0.155%
PMMA/RhB/FUR5	FUR	5%	0.155%

2.3 Characterisation of frustules

2.3.1 FT-IR and SEM analyses

Chemical properties of DE and FUR frustules were assessed using Fourier Transform Infrared Spectroscopy (FTIR, *Perkin Elmer 100*). The spectra were collected over the range 4000-400 cm^{-1}, by averaging 32 scans at a maximum resolution of 4 cm^{-1}.

The microstructure of both type of frustules was investigated by means of Field Emission Scanning Electron Microscopy (FE-SEM, *Leo Supra 35*).

2.3.2 Frustule photoluminescence analyses

PL properties of FUR and DE frustules were microscopically investigated. 1% (w/w) Frustule suspensions were analysed using an *Olympus FV1000* Confocal Laser Scanning Microscope (CLSM), 60x NA 1.42, oil objective, by means of spectral analysis (SA). SA measured emitted light intensities at intervals of 5 nm across the total spectrum and generated curves via intensity profiles. At least 10 valves per sample were analysed under laser excitation: diode laser (405 nm), Argon laser (488 and 515 nm), diode laser (559 nm) and Helium Neon laser (635 nm). Emission spectra were acquired using 2D reconstructions of valves after optical sectioning of the Region Of Interest (ROI, step size 1 µm), background signal, due to the glass slide, was calculated and subtracted from the final spectra.

2.4 Characterisation of random lasers based on frustules as scatterers

2.4.1 Microstructure

The microstructure of composite films was investigated by means of FE-SEM (*Leo Supra 35*).

2.4.2 Random laser experiments

The dye fluorescence was measured at room temperature by using the frequency doubled output (532 nm) of a 10 Hz, Q-switched Nd: YAG laser as excitation source. The pump pulse duration was 6 ns. A half-wave plate and a Glan-Taylor polarizer prism are used to control the laser power, which has been measured with an energy meter. The laser spot area on the sample was 16 mm^2. The emission was collected in front configuration with a fiber-bundle trough a lens and analyzed by a high-resolution spectrometer (OceanOptics HR4000).[31]

3. Results and discussion

3.1 FT-IR and SEM analyses of frustules

The FTIR spectra of DE and FUR frustules are reported in **Fig. 1**.

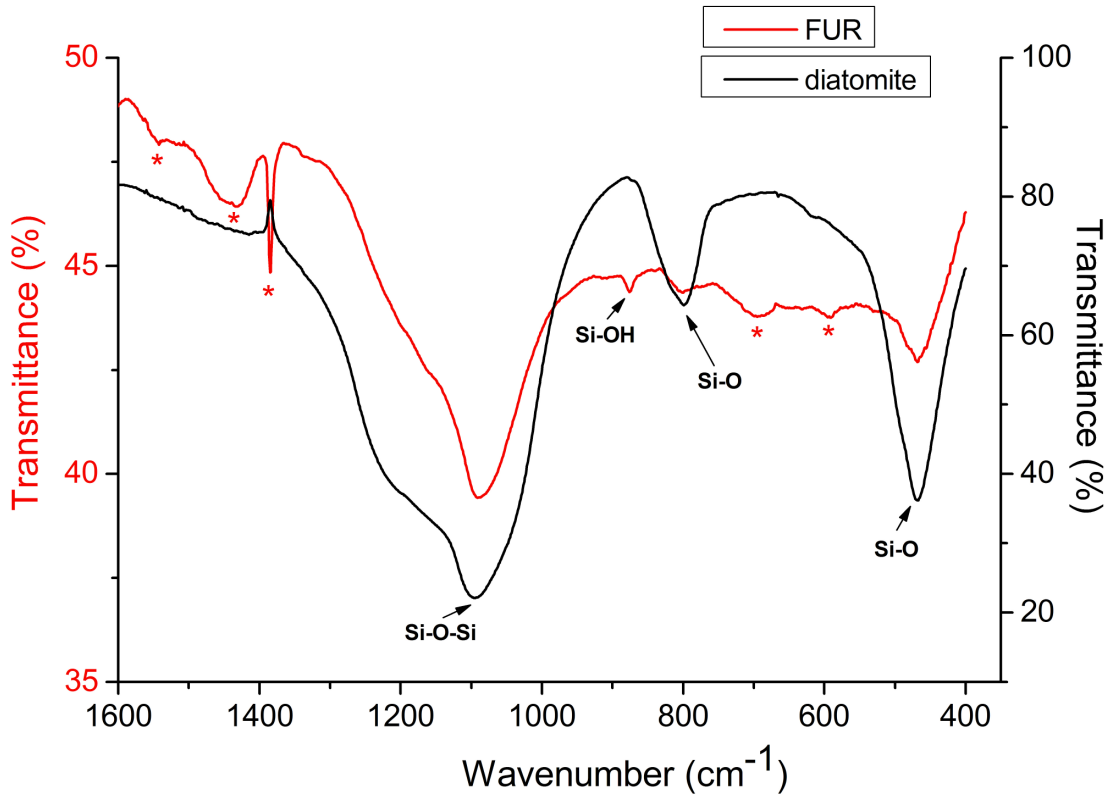

Fig. 1 FT-IR spectra of diatomite and biofilm frustules (FUR).

Both samples show the same three characteristic broad bands at 1095, 799 and 468 cm^{-1}. The band detected at 1095 cm^{-1} is assigned to Si-O-Si anti-symmetric stretching mode.[32] The absorption around 799 cm^{-1} can be attributed to Si-O bending vibration.[33] The absorption at 468 cm^{-1} is characteristic of the Si-O-Si framework. In detail this band corresponds to Si-O rocking vibration where the oxygen atom moves perpendicular to the Si-O-Si plane.[33] There are other peaks in the spectrum of FUR frustules. Particularly, the absorption around 875 cm^{-1} corresponds to Si-OH vibration.[33,34] The silica surface in fact contains silanol groups that act as centres for adsorption through forming hydrogen bonds with many polar organic compounds or reaction with various functional groups.[35] Therefore these functional groups can play an important role in the polar dye adsorption (RhB) which is also dependent on the pore structure. The absence of these groups in the diatomite sample can be due to the thermal treatment carried out by the manufacturer to purify the product. The other bands detected in the spectrum of FUR frustules could be probably associated to

residual organic components such as peptides (long-chain polyamines (LCPAs) and silaffins), chitin polymers and/or glucosidic molecules, probably closely attached or even embedded into diatom cell walls.[36,37] In detail, the absorptions around 1540, 1438 and 694 cm^{-1} can be attributed to chitin. The band detected at 1540 cm^{-1} corresponds to the N-H bending of amide II, the absorption around 1438 cm^{-1} can be associated to a symmetrical deformation of CH_3 groups of amide III and the band at 694 cm^{-1} can be attributed to OH out of plane bending.[38,39] SEM images of DE and FUR frustules are shown in **Figs. 2 and 3**, respectively.

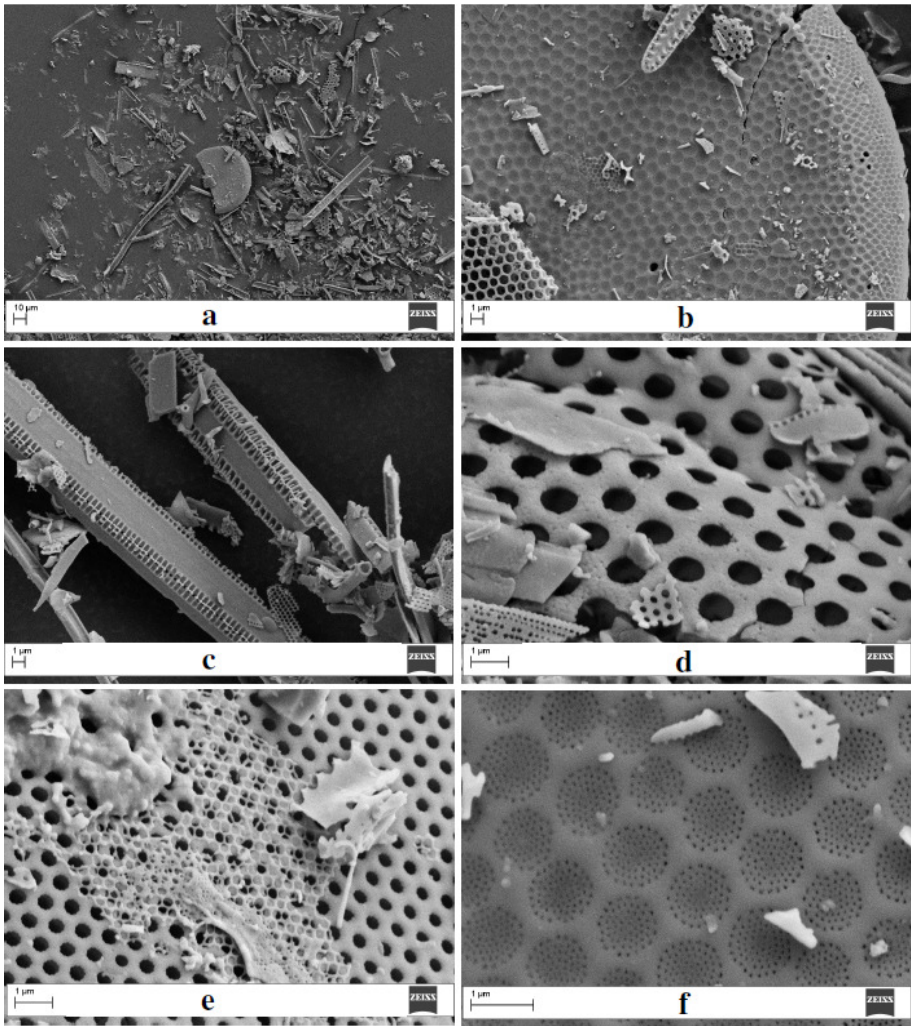

Fig. 2 SEM micrographs of diatomite.

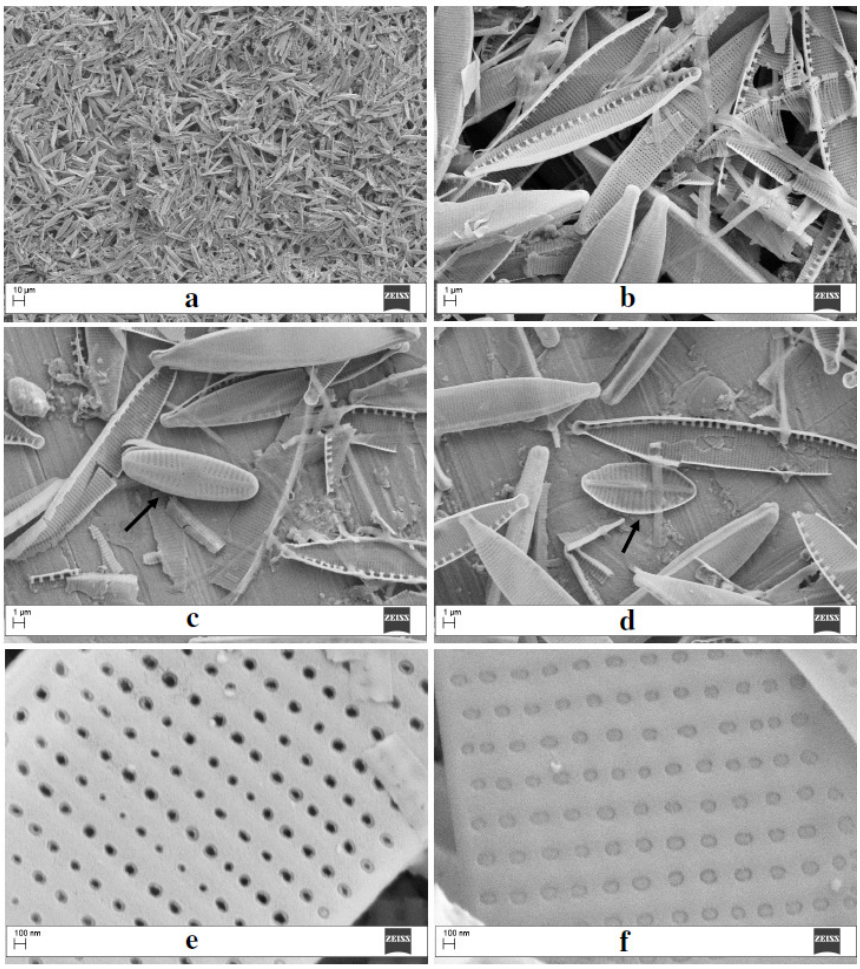

Fig. 3 SEM micrographs of biofilm frustules (FUR).

The diatomite sample is heterogeneous, being composed of frustules more or less fragmented belonging to a variety of different species of both centric and pennate diatoms displaying different size and morphology. Rectangular and circular pores with size ranging from 25 nm to 1 μm were observed on most of fragments. Conversely, FUR sample was more homogeneous with a dominant frustule type, that of *Nitzschia palea* var. *minuta*. Less abundant were frustules of the diatoms *N. amphibia, N. umbonata and Eolimna subminuscola*. Overall, the length of frustules obtained from biofilm was about 20 μm with pore diameters ranging between 20 and 100 nm.

Moreover some pores appeared occluded and probably did not contribute to the scattering of light.

3.2 Photoluminescence of DE and FUR frustules

PL data of FUR and DE frustules by SA allowed to evaluate if biosilica intrinsic features could have affected the random laser emission observed in this study. In fact, PL between 460 and 560 nm has been reported for the frustules of seven diatom genera, after excitation with UV light, in the range of 325-385 nm.[40-43] In this study, SA revealed PL in FUR frustules after excitation at λ_{ex} 488

nm, with an emission peak at $\lambda_{em.max}$ 508 nm (**Fig. 4** (a)). Emission signals were also recorded after excitation at λ_{ex} 515, 543 and 635 nm with $\lambda_{em.max}$ at 528, 553 and 651 nm, respectively (**Fig. 4** (b-d)); whilst no PL was recorded at λ_{ex} 405 nm. By contrast, DE frustules showed emission only at λ_{ex} 405 nm (**Fig**. **4**(e)). These different PL properties of the two types of biosilica investigated could be due to differences in the surface properties of FUR and DE frustules, such as silanol groups and pore patterns. Further analyses are required in order to better understand the effects of the physical and chemical characteristics of the studied biosilica on the PL properties here evidenced.

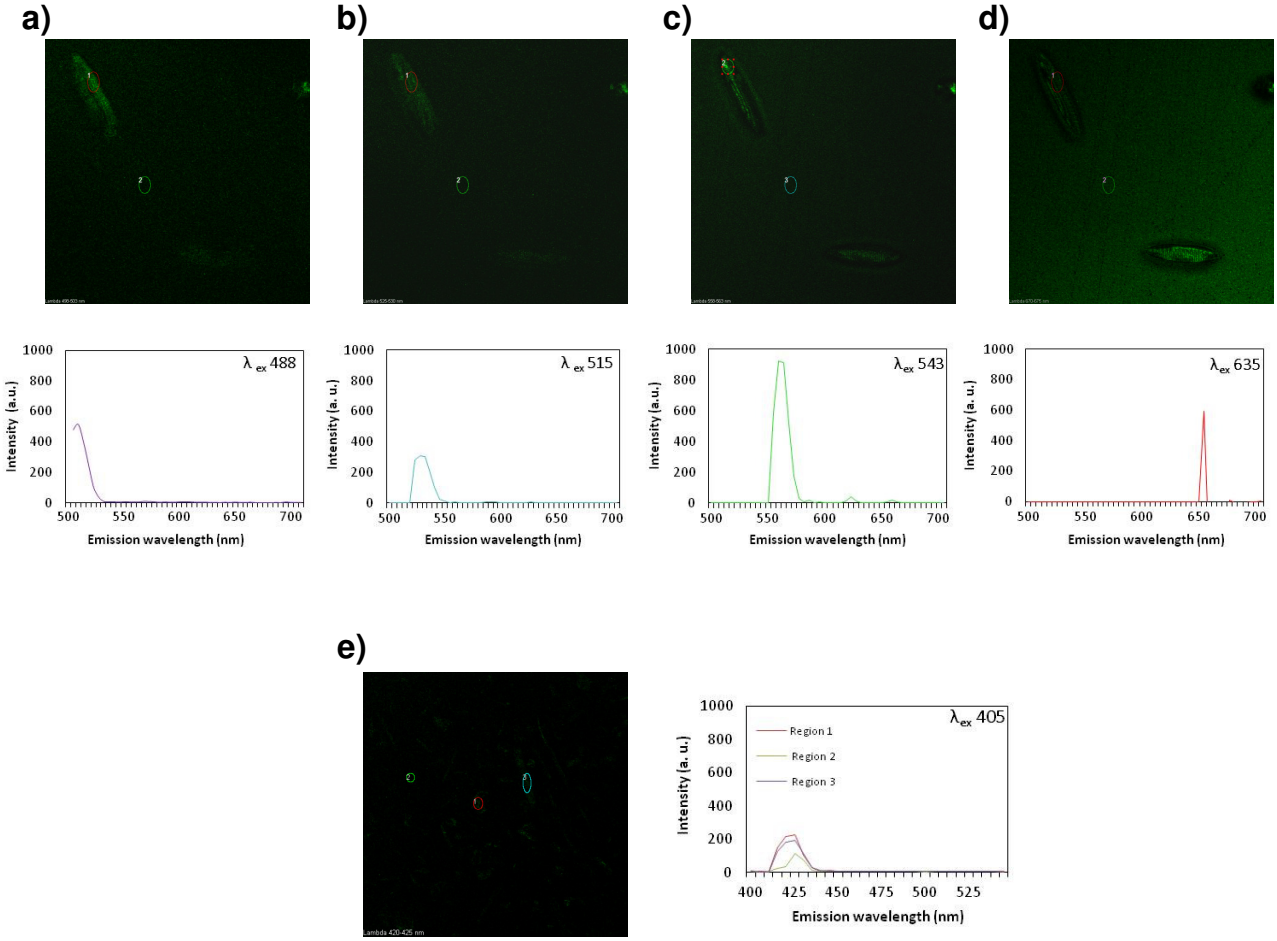

Fig. 4 FUR (a-d) and DE (e) 2D images of frustules and relative emission spectra of the ROIs selected.

3.3 Microstructure of polymer composite random lasers

SEM observations of the cross-sections of the PMMA/RhB matrix composites filled with DE and FUR showed that both types of frustules are uniformly dispersed in the polymer matrix but the matrix/filler adhesion is not optimal (**Fig. 5**). Moreover some pores seem to be filled by the polymer.

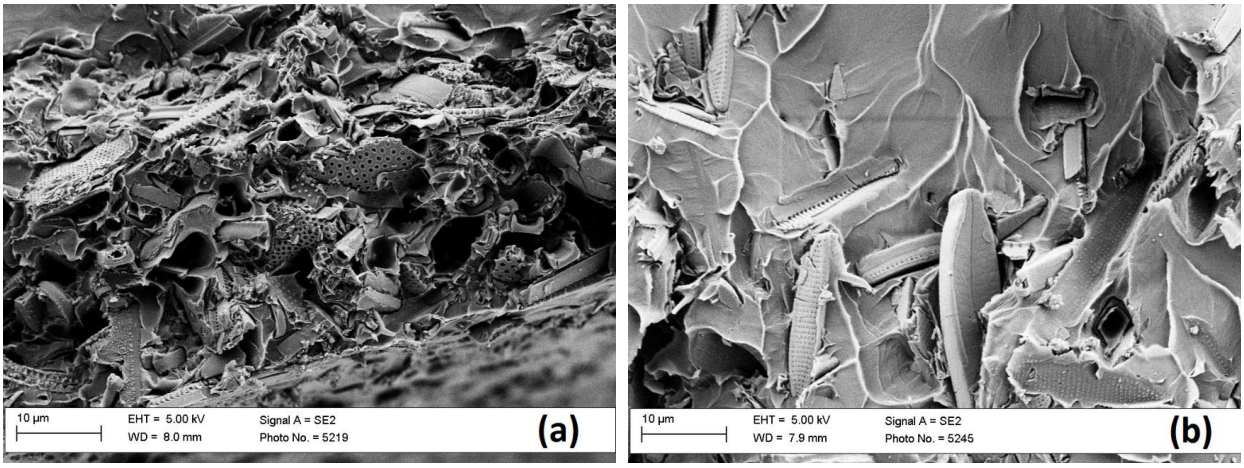

Fig. 5 SEM micrographs of the cross-sections of PMMA/RhB matrix composites filled with diatomite (PMMA/RhB/DE5 sample) (a) and FUR (PMMA/RhB/FUR5 sample) (b).

3.4 Random laser experiments

In the random laser experiments the emission spectra of the samples were collected in the wavelength range 540 -700 nm exciting the samples with λ = 532 nm and increasing gradually the pump energies. The normalised emission spectra of the PMMA/RhB/DE20 sample measured at different pumping energies (indicated in figure) are reported in **Fig. 6**.

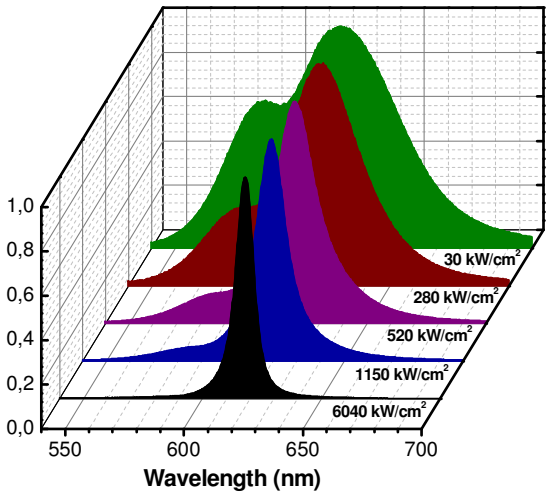

Fig. 6 Normalised PL spectrum of the PMMA/RhB/DE20 sample at different excitation power density (the values are reported in the figure).

At low pumping energy the sample emission is characterised by the spontaneous emission of the RhB dye. This is a broad-band spectrum with a double structure presenting the maximum peak position at 614 nm with FWHM of 70 nm. With increasing the pumping energy a spectral narrowing (centered at 575 nm) was observed, indicating the onset of an amplified spontaneous emission process (ASE) due to a random lasing effect. For the other samples with different DE concentration the behaviour is qualitatively the same, but the quantitative values are different as reported in the following. The dependence of the laser threshold on the density of scattering particles has been reported by many authors as a clear signature of the fact that the laser feedback in the material is related to scattering and of a RL effect.[44,45,25]

In **Fig. 7** is showed the power dependency of the peak intensity (input-output characteristic) and the emission peak FWHM of the PMMA/RhB/DE composite materials with different DE concentrations.

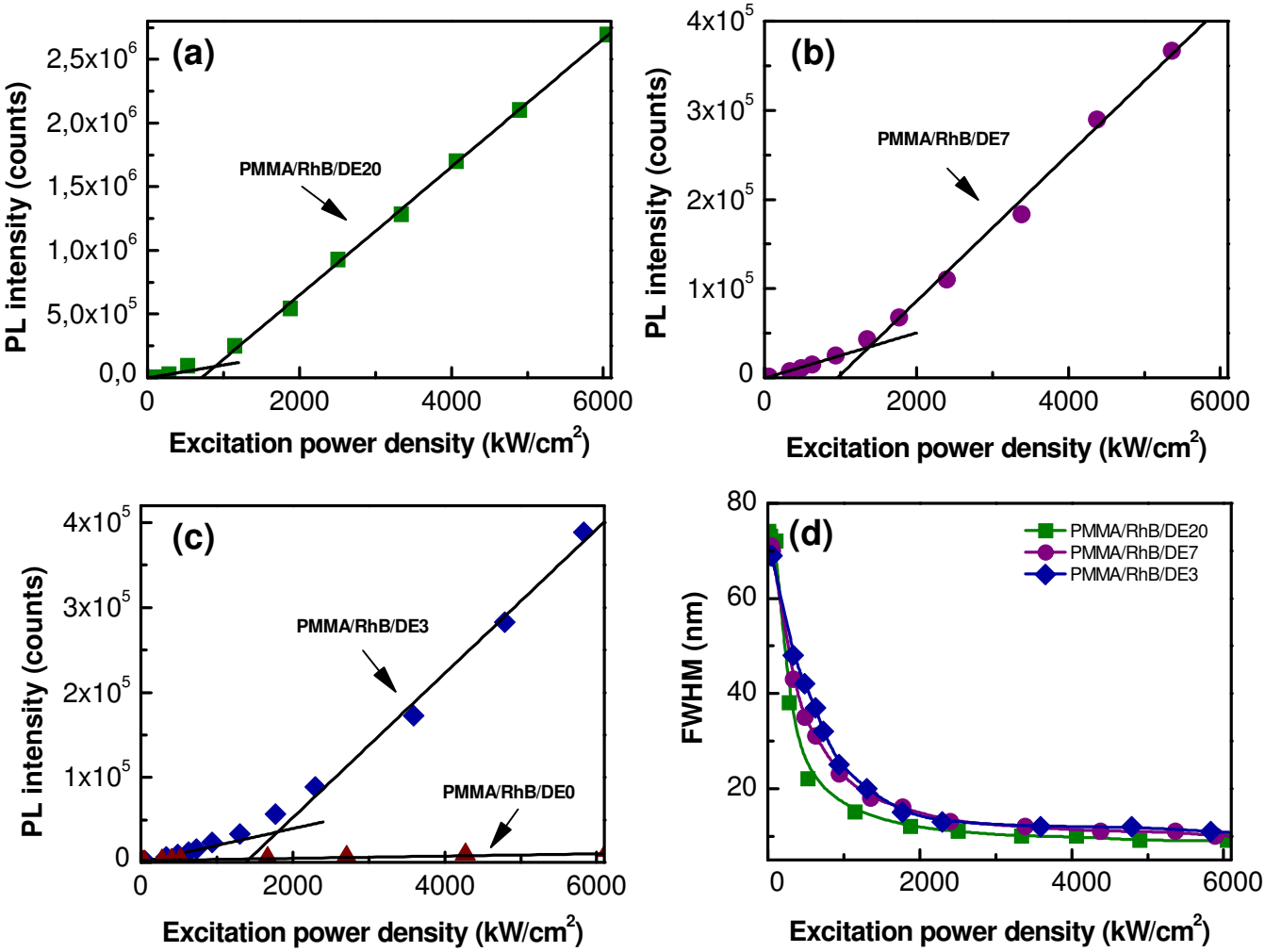

Fig. 7. Power dependency of the peak intensity (a-c) and the FWHM (d) of the PMMA/RhB/DE composite materials with different DE concentrations.

The power dependency of the peak intensity showed the onset of a non-linear response in the RhB /DE co-doped material at all the DE concentrations tested, while the sample doped only with the chromofore showed the expected linear response and no band narrowing was observed. This is an evidence that the presence of DE in the composite material is responsible of the strong scattering of the light, which provides the required feedback mechanism for random lasing.

The **Fig. 7 (c)** shows the input-output response of the PMMA/RhB/DE0 and PMMA/RhB/DE3. For the first sample the data can be fitted with a single linear law, while for the second sample the low power and high power branch of the graphs can be fitted with different linear laws (fit confidence R^2=0.99) showing a clear change in the slope of the input-output response. Such effect is much more evident with increasing the DE concentration in the sample (**Fig. 7 (a,b)**). In the case of a random laser material the threshold of the process can be estimated as the intercept of the input-output curves (high power branch) with the horizontal axes. Consistently with the interpretation of the observed spectral narrowing as a random laser effect, the laser threshold depends on the scatterer concentration. Such threshold diminishes with increasing the DE concentration in the composite, with the lowest threshold value of 712 kW/cm^2 for the PMMA/RhB/DE20 composite (**Table 2**).

Table 2
Random laser threshold for the sample with different DE (%) concentration.

Sample	Threshold (kW/cm^2)
PMMA/RhB/DE0	NO
PMMA/RhB/DE3	1380
PMMA/RhB/DE7	963
PMMA/RhB/DE20	712

In an equivalent determination of the laser threshold the band narrowing was studied as a function of the pump power. At low power the FWHM is almost constant for all the DE concentration, but at the onset of the ASE process it results in a rapid and consistent decrease until a saturation value is reached (down to 8 nm in the PMMA/RhB/DE20 sample).

The laser threshold by FWHM can be estimated as the median value between the initial width of the emission band and its final saturation value. In this case a close correspondence between the threshold estimated with the two methods was found, consistent with the results of similar experiments in Rhodamine 6G dye and TiO_2 nanoparticles (NPs) blends.[46]

The experiment showed that above a certain pumping threshold the dye emission band narrows as a whole close to a preferential frequency corresponding to the maximum of the gain spectrum. As reported before such behaviour is typical of an intensity feedback mechanism, the so-called incoherent random lasing effect, whereas a coherent feedback would have resulted in a series of extremely sharp emission peaks at some resonant frequencies. It is known that by increasing the particles concentrations in a random media such as a liquid suspension of particles or a polymer host a transition from the incoherent to the coherent feedback mechanism can be observed.[22] This requires that the transport mean free path, that is the average distance a photon travels in between two consecutive scattering events, approaches the optical wavelength.

In the examined case most of the frustules are in a size range that is an order of magnitude above the visible optical wavelengths. Thus, some coherency may arise from the scattering between the pore structures of DE whose size is in the range of 10 nm-1 μm, but any transition could be observed considering that the average pore density in the composite, also using a filler content up to 20%, is not high enough. Moreover some pores are filled up by the PMMA as observed with SEM microscopy (**Fig. 5**).

The low power emission of the PMMA/RhB/FUR5 sample is reported in **Fig. 8**. The low power emission spectrum of the RhB dye in the PMMA/RhB/DE20 sample is also reported for comparison.

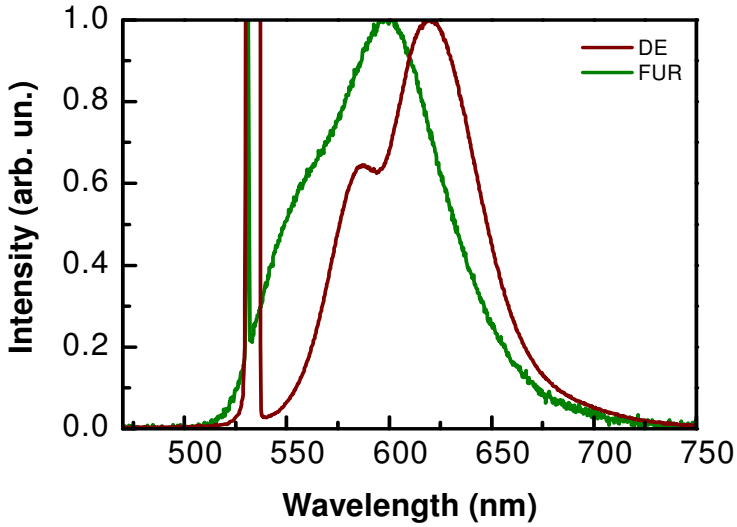

Fig. 8 Low power emission spectrum of the PMMA/RhB/FUR5 composite material (green line) compared with the emission of PMMA/RhB/DE20 sample at the same excitation power density of 30 kW/cm^2 (brown line).

For the FUR doped sample the low power emission band was slightly different with respect to the sample doped only with the dye or co-doped with the DE. In detail, the band was less resolved and shifted to lower wavelength. Such effect should be due to intrinsic properties of the frustules. FUR frustules, in fact, contain several binding sites for the dye (i.e. superficial silanol groups, and residual organic components detected by FT-IR analyses). Therefore a modification of the emission spectrum could arise from possible chemical interaction between RhB and these binding sites. Moreover the frustules PL emission spectra recorded with the confocal microscope set-up showed that the FUR frustules displays their own emission, in close correspondence with the shoulder observed on the short wavelengths side of the spectrum (**Fig. 4 (c)**).

For the case of the PMMA/RhB/FUR5 emission, with increasing the excitation power density a spectral narrowing centered at 602 nm is observed, with low threshold of 308 kW/cm^2. However the emission intensity saturates at a quite lower power (less than 4000 kW/cm^2) respect to the DE doped composites, and presents a FWHM of 20 nm (**Fig. 9 (a,b)).**

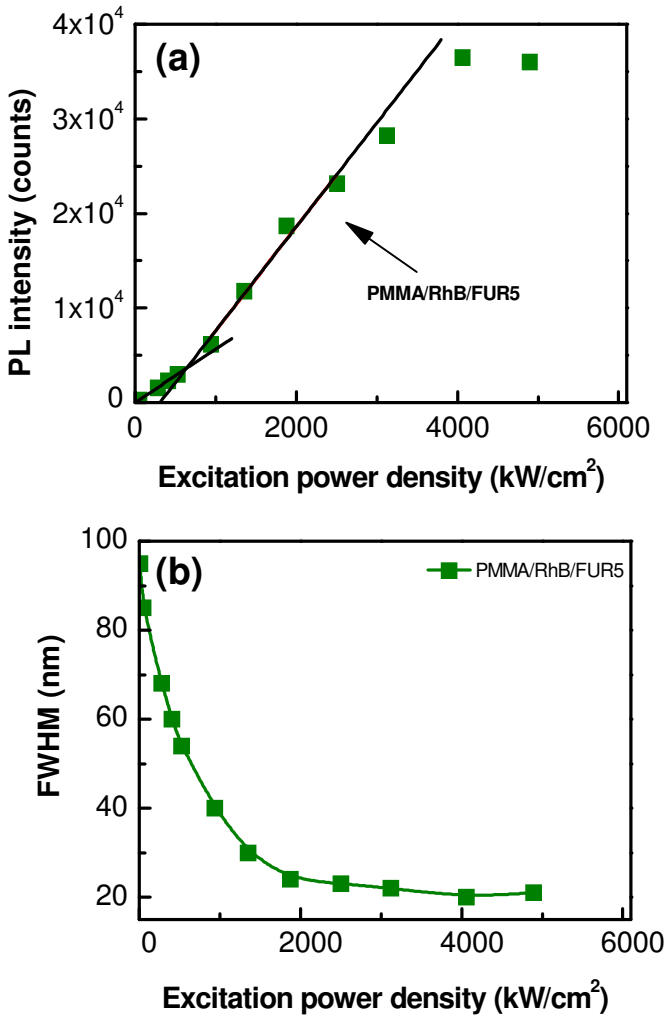

Fig. 9 Power dependency of the peak intensity (a) and the FWHM (b) of the PMMA/RhB/FUR5 sample.

The FUR doped sample presents a prevalence of frustules with a selected size and elongated shape with 20 micron length.

The concentration of 5% was dictated by the amount of material available, since this is a field collected sample and all the available material was used except the little amount saved for the confocal microscope investigation. Such concentration is in the range of the ones tested for the DE, and it is lower than the maximum concentration tested for the DE, which was the 20%.

Interestingly, in this species-specific sample the RL effect occurs with a lower threshold respect to all the DE doped ones.

A possible reason, and an appealing one, is that in the case of the biofilm frustules the process is assisted by the onset of morphology dependent resonances. In fact the diatom size is in the range of most typical morphology-dependent resonators.[21] Further investigations are needed to clarify this hypothesis like testing different diatom species with a variety of sizes and shapes in order to assess the effects of frustules morphology on the RL effect. On the other hand, the FUR sample reaches the saturation at lower pumping intensity respect to the DE doped ones. This is probably due to the frustule intrinsic fluorescence emission and other non-radiative recombination channels that quenches the radiative emission. Also the presence of organic residuals could cause the quenching. The different behaviour of DE and FUR can also be due to the different porosity and superficial pore distribution and size. Probably, in FUR frustules characterised by less porosity and smaller pore size, the RhB content employed was too much. Dye molecules, entering into these narrow pores, could get in close contact with each other leading to a possible formation of clusters or small crystals, which affect negatively the lasing action. Also the possible chemisorption of RhB on the surface of the FUR frustules through silanol group and/or organic impurity could cause the formation of small crystals. Probably, reducing the dye content, eliminating the organic residuals and reducing the luminescence activity of frustules related to the superficial silanol groups, the observed saturation at lower pumping intensity with respect to the DE doped ones could not occur. Summarizing FUR frustules are promising materials as scatterers in a random laser since RL effect occurs with a lower threshold respect to DE and the more controlled shape and pore size with respect to DE could lead to a better reproducibility of the realised random laser.

4. Conclusions

In this work two types of diatom frustules (diatomite and biofilm frustules) were used as scatterers in PMMA matrix composite Random Lasers containing RhB as gain medium. Diatomite consisted on mixed species of frustules with no specific shape and size and with a pore size ranging from 25 nm to 1 μm. Biofilm frustules had elongated shape with 20 micron length and pore diameters

ranging between 20 and 100 nm. PL of frustules obtained from biofilm was higher with respect to diatomite probably due to presence of superficial silanol groups. An incoherent random lasing effect was observed in all prepared polymer composites. It was found that the laser threshold depend on the kind of frustule and diminishes with increasing amount of the frustules. The lowest value was reached using biofilm frustules (308 kW/cm^2) probably because of the size of this species-specific biosilica, which is in the range of most typical morphology-dependent resonators. On the other hand, using this type of frustules the random laser reaches the saturation at lower pumping intensity with respect to the case of employing diatomite. This behaviour is probably associated to the frustule luminescence related to the superficial silanol groups and other non-radiative recombination channels that quenches the radiative emission. Probably, reducing the frustule intrinsic fluorescence, the observed saturation at low pumping intensity could not occur. On these grounds biofilm frustules are promising materials as scatterers in a random laser since RL effect occurs with a lower threshold respect to diatomite and the more controlled shape and pore size with respect to DE could lead to a better reproducibility and modulation of the random lasers.

Notes and references

1 K. S. A.Butcher, J. M. Ferris and M. R. Phillips, *Sensor Actuator,* 2003, 6.

2 C. E. Hamm, R. Merkel, O. Springer, P. Jurkojc, C. Maier, K. Prechtel and V. Smetacek, *Nature*, 2003, **421**, 841.

3 M. De Stefano, L. De Stefano and R. Congestri, *Superlattice. Microst*., 2009, **46**, 64.

4 G. Di Caprio, G. Coppola, L. De Stefano, M. De Stefano, A. Antonucci, R. Congestri and E. De Tommasi, *J. Biophotonics*, 2014, **7**, 341.

5 M. A. Ferrara, P. Dardano, L. De Stefano, I. Rea, G. Coppola, I. Rendina, R. Congestri, A. Antonucci, M. De Stefano and E. De Tommasi, *PLOS One*, 2014, **9**, e103750.

6 C. Wang, S. Yu, W. Chen and C. Sun, *Sci. Rep.,* 2013, **3**, 1025, DOI: 10.1038/srep01025.

7 Y. Wang , J. Cai, Y. Jiang, X. Jiang and D. Zhang, *Appl. Microbiol. Biotechnol*., 2013, **97**, 453.

8 J. Toster, K. S. Iyer, W. Xiang, F. Rosei, L. Spiccia and C. L. Raston, *Nanoscale*, 2013, **5**, 873.

9 E. Van Eynde, T. Tytgat, M. Smits, S. W. Verbruggen, B. Hauchecorne and S. Lenaerts, *Photochem. Photobiol. Sci.*, 2013, **12,** 690.

10 Y. Lang, F. D. Monte, B. J. Rodriguez, P. Dockery, D. P. Finn and A. Pandit, *Sci. Rep*., 2013, **3** 3205.

11 Z. Bao, M. R. Weatherspoon, S. Shian, Y. Cai, P. D. Graham, S. M. Allan, G. Ahmad, M. B. Dickerson; B. C. Church, Z. Kang, H. W. Abernathy, C. J. Summers, M. Liu, and K. H. Sandhage,

Nature, 2007, **446**, 172.

12 S. Lettieri, A. Setaro, L. De Stefano, M. De Stefano and P. Maddalena, *Adv. Funct. Mater.*, 2008, **18**, 1257.

13 S. N. Olof, J. A. Grieve, D. B. Phillips, H. Rosenkranz, M. L. Yallop, M. J. Miles, A. J. Patil, S. Mann and D. M. Carberry, *Nano Lett*., 2012, **12**, 6018.

14 N. V. Arteaga-Larios, Y. Nahmad, H. R. Navarro-Contreras, A. Encinas and J. Viridiana García-Meza, *Luminescence*, 2014, DOI: 10.1002/bio.2646.

15 T. V. Ramachandra, D. M. Mahapatra, K. B and R. Gordon, *Ind. Eng. Chem. Res.,* 2009, **48**, 8769.

16 R. Gordon, D. Losic, M. A. Tiffany, S. S. Nagy and FA. Sterrenburg, *Trends Biotechnol.*, 2009, **27** 116.

17 M. Hildebrand, A. K. Davis, S. R. Smith, J. C. Traller and R. Abbriano, *Biofuels*, 2012, **3**, 221.

18 P. Boelen, R. van Dijk, J. S. Sinninghe Damsté, WI Rijpstra and AG. Buma, *AMB Express*, 2013, **3**, 26.

19 S. Gottardo, R. Sapienza, P. D. Garcia, A. Blanco, D. S. Wiersma and C. Lopez, *Nat. Photonics*, 2008, **2**, 429.

20 D. S. Wiersma, *Nat. Phys*., 2008, **4**, 359.

21 N. M. Lawandy, R. M. Balachandran, A. S. L. Gomes and E. Sauvain, *Nature*, 1994, 368, 436.

22 H. Cao, J. Y. Xu, S.-H. Chang and S. T. Ho, *Phys. Rev. E*, 2000, **61**, 1985.

23 V. M. Markushev, V. F. Zolin and Ch. M. Briskina, *Sov. J. Quantum Electron.,* 1986, **16**, 281.

24 M. A. Noginov, N. E. Noginova, H. J. Caulfield, P. Venkateswarlu, T. Thompson, M. Mahdi and V. Ostroumov, *JOSA B*, 1996, **13**, 2024.

25 R. M. Balachandran and N. M. Lawandy, *Opt. Lett*., 1996, **21**, 1603.

26 H. Cao, *Wave Random Media*, 2003, **13**, R1.

27 W. Yang, P. J. Lopez and G. Rosengarten, *Analyst.*, 2011, **136**, 42.

28 P. V. Vasconcelos, J. A. Labrincha and J. M. F. Ferreira, *J. Eur. Ceram. Soc.*, 2000, **20**, 201.

29 R. Congestri, E. J. Cox, P. Cavacini and P. Albertano, *Diatom Res.*, 2005, **20**, 241.

30 R. Congestri, F. Di Pippo, R. De Philippis, I. Buttino, G. Paradossi and P. Albertano, *Aquat. Microb. Ecol.*, 2006, **45** 301.

31 A. Yadav, R. De Angelis, M. Casalboni, F. De Matteis, P. Prosposito, F. Nanni and I. Cacciotti, *Opt. Mater.*, 2013, **35**, 1538.

32 E. Gulturk and M. Guden, *JAMME*, 2011, **46**, 196.

33 N. D. Singho and M. R. Johan, *Int. J. Electrochem. Sci.*, 2012, **7**, 5604.

34 M.-C. Wua, J. J. P. Coca, G. R.-L. Chang, S.-Y. Suen, C.-F. Lin, H.-N. Chou, S.-Y. Lai and M.-Y. Wang, *Process Biochem.*, **2012**, 47, 2204.

35 M. A. M. Khraisheh, M. A. Al-Ghouti, S. Allen and M. Ahmad, *Water Res.*, 2005, **39**, 922.

36 R. Hedrich, S. Machill, E. Brunner, *Carbohyd. Res.*, 2013, **365**, 52.

37 C. A. Durkin, T. Mock, E. V. Armbrust, *Eukaryot. Cell*, 2009, **8**, 1038.

38 I. F. M. Rumengan, E. Suryanto, R. Modaso, S. Wullur, T. E. Tallei and D. Limbong, *Int. J. Fish. Aquat. Sci.*, 2014, **3**, 12.

39 K. Prabu, E. Natarajan, *Adv. Appl. Sci. Res.,* 2012, **3**, 1870.

40 K. S. A. Butcher, J. M. Ferris, M. R. Phillips, M. Wintrebert-Fouquet, J. W. Jong Wah, Nemanja Jovanovic, W. Vyverman and V. A. Chepurnov, *Mater. Sci. Eng. C*, 2005, **25**, 658.

41 L. De Stefano, L. Rotiroti, M. De Stefano, A. Lamberti, S. Lettieri, A. Setaro and P. Maddalena, *Biosens. Bioelectron.*, 2009, **24**, 1580.

42 B. Goswami, A. Choudhury and A. K. Buragohain, *Luminescence*, 2012, **27**, 16.

43 M. Kucki and T. Fuhrmann-Lieker, *J. R. Soc. Interface*, 2012, **9**, 727.

44 N. M. Lawandy and R. M. Balachandran, *Nature*, 1995, **373**, 203.

45 W. Zhang, N. Cue and K. M. Yoo, *Opt. Lett.*, 1995, **20**.

46 J. Kitur, G. Zhu, M. Bahoura and M. A. Noginov, *J. Opt.*, 2010, **12**, 024009.